ALMA MATER STUDIORUM
UNIVERSITÀ DI BOLOGNA

ARCHIVIO ISTITUZIONALE
DELLA RICERCA

Alma Mater Studiorum Università di Bologna
Archivio istituzionale della ricerca

77 % Photothermal Conversion in Blatter-Type Diradicals: Photophysics and Photodynamic Applications

This is the final peer-reviewed author's accepted manuscript (postprint) of the following publication:

Published Version:
Ji Y., Moles Quintero S., Dai Y., Marín-Beloqui J.M., Zhang H., Zhan Q., et al. (2023). 77 % Photothermal Conversion in Blatter-Type Diradicals: Photophysics and Photodynamic Applications. ANGEWANDTE CHEMIE. INTERNATIONAL EDITION, 62(42), 1-8 [10.1002/anie.202311387].

Availability:
This version is available at: https://hdl.handle.net/11585/947097 since: 2023-10-31

Published:

DOI: http://doi.org/10.1002/anie.202311387

Terms of use:

Some rights reserved. The terms and conditions for the reuse of this version of the manuscript are specified in the publishing policy. For all terms of use and more information see the publisher's website.

This item was downloaded from IRIS Università di Bologna (https://cris.unibo.it/).
When citing, please refer to the published version.

(Article begins on next page)

09 November 2026

This is the final peer-reviewed accepted manuscript of:

[Y. Ji, S. Moles Quintero, Y. Dai, J. M. Marín-Beloqui, H. Zhang, Q. Zhan, F. Sun, D. Wang, X. Li, Z. Wang, X. Gu, F. Negri, J. Casado, Y. Zheng "77% Photothermal Conversion in Blatter-Type Diradicals: Photophysics and Photodynamic Applications", Angew. Chem. Int. Ed. 2023, 62, e202311387 **]**

The final published version is available online at: **[https://doi.org/10.1002/anie.202311387]**

Terms of use:

Some rights reserved. The terms and conditions for the reuse of this version of the manuscript are specified in the publishing policy. For all terms of use and more information see the publisher's website.

This item was downloaded from IRIS Università di Bologna (https://cris.unibo.it/)

When citing, please refer to the published version.

77% Photothermal Conversion in Blatter-Type Diradicals: Photophysics and Photodynamic Applications

Yu Ji,[a] Sergio Moles Quintero,[b] Yasi Dai,[c] Jose M. Marín Beloqui,[b] Hanjun Zhang,[a] Qian Zhan,[a] Fanxi Sun,[a] Dongsheng Wang,*[a] Xiangkun Li,[d] Zhiyi Wang,[d] Xinggui Gu,[e] Fabrizia Negri,[c] Juan Casado*[b] and Yonghao Zheng*[a,f]

[a] Y. Ji, H. Zhang, Q. Zhan, F. Sun, Prof. D. Wang, Prof. Y. Zheng
School of Optoelectronic Science and Engineering
University of Electronic Science and Technology of China (UESTC)
Chengdu 610054, People's Republic of China
E-mail: zhengyonghao@uestc.edu.cn, wangds@uestc.edu.cn

[b] S. Quintero, J. Beloqui, J. Casado
Department of Physical Chemistry
University of Málaga
Campus de Teatinos s/n, Málaga 29071, Spain
E-mail: casado@uma.es

[c] Y. Dai, F. Negri
A Dipartimento di Chimica 'Giacomo Ciamician'
Università di Bologna
Via F. Selmi, 2, 40126 Bologna, Italy and ISTM, UdR, Bologna, Italy

[d] X. Li, Prof. Z. Wang
Spin-X Institute, School of Chemistry and Chemical Engineering
South China University of Technology
Guangzhou 510641, People's Republic of China

[e] Prof. X. Gu
Beijing Advanced Innovation Center for Soft Matter Science and Engineering, College of Materials Science and Engineering, State Key Laboratory of Chemical Resource Engineering
Beijing University of Chemical Technology
Beijing 100029, People's Republic of China

[f] Prof. Y. Zheng
State Key Laboratory of Organic Electronics and Information Displays & Institute of Advanced Materials(IAM), Nanjing University of Posts & Telecommunications, 9 Wenyuan Road, Nanjing 210023, People's Republic of China.

Supporting information for this article is given via a link at the end of the document.

Abstract: Diradicals based on the Blatter units and connected by acetylene and alkene spacers have been prepared. All the molecules show sizably large diradical character and low energy singlet-triplet energy gaps. Their photo-physical properties concerning their lowest energy excited state have been studied in detail by steady-state and time-resolved absorption spectroscopy. We have fully identified the main optical absorption band and full absence of emission from the lowest energy excited state. A computational study has been also carried out that has helped to identify the presence of a conical intersection between the lowest energy excited state and the ground state which produces a highly efficient light-to-heat conversion of the absorbed radiation. Furthermore, an outstanding photo-thermal conversion near 80% has been confirmed, close to the highest in the diradicaloid field. For the first time, stable diradicals are applied to photo-thermal therapy of tumor cells with good stability and satisfactory performance at near-infrared region.

Introduction

The electronic structure of singlet diradicaloids is described by the existence of four lower energy-lying electronic states that emerge as a result of the electronic configurational mixing between the open-shell covalent diradical and the closed-shell ionic configurations (Scheme 1).[1] This makes the ground electronic state (GR) to be an admixture of the two, with contributions in proportions that can be tuned by chemical functionalization.

On the other hand, the excited state associated with the above mixing has larger ionic portions and the same symmetry as the GR by which is an optically dark state (DR). Furthermore, for molecules with medium-large diradical character, the DR state becomes the lowest singlet excited state, S_1. The other two states are: i) the pure ionic state that has different orbital symmetry than

This item was downloaded from IRIS Università di Bologna (https://cris.unibo.it/)

When citing, please refer to the published version.

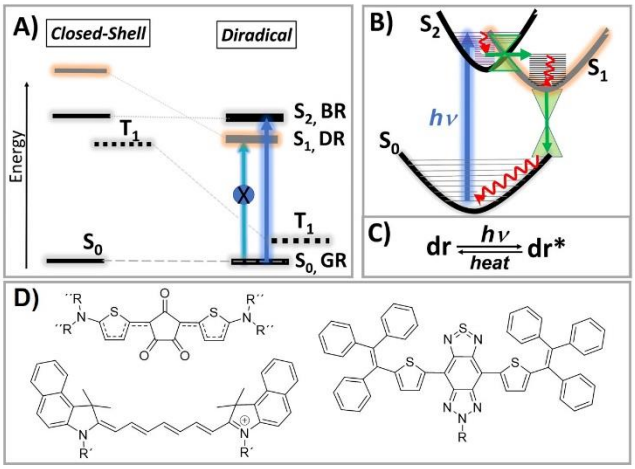

Scheme 1. (A) Four energy lying electronic states of diradicals and their evolution with the configurational mixing from the closed-shell situation. (B) Main photophysical events in diradicals between the main electronic states: blue arrow is light absorption; red arrows are vibrational relaxation and green arrows are for conical intersections (CI). (C) Light-to-heat photoconversion process (dr: diradicals). (D) Some examples of small organic molecules in photothermal conversion energy (PCE) actuation. Upper-left: molecule with very weak diradical character (R, R´ and R´´ are different alkyl chains); Bottom-left: cyanine-based molecule; Bottom-right: closed shell molecule with donor-acceptor-donor pattern.

the GR and is optically active (BR). For medium-large diradical character systems, the BR state is the second excited state singlet, S_2. And ii) the first triplet state (T_1) which is lying very close in energy to the GR making it available for thermal low-spin to high-spin transitions (Scheme 1).[1] The inherent ionic character of the BR state makes the GR→BR transitions to accumulate strong oscillator strength and it is associated with electronic absorption bands that display large absorbance (giving rise to the main absorption bands of diradicals) and acting as excellent radiation absorber molecules and materials. In general, diradicals are receiving much current attention because their potential applications in several organic electronic applications such as in ambipolar field effect organic transistors, in photovoltaics as near-infrared (NIR) sensors and diodes, as well as in spintronics devices due to their magnetic responsive properties.[2-6] Finally, the ability to combine strong light absorption properties with efficient light-to-heat conversion (i.e., photothermal conversion efficiency, or PCE) further dressed with the property of having thermally accessible high-spin triplet states might certainly result in powerful candidates for photodynamic mechanisms.[7-9] In this article, we hypothesize that strong absorption light energy by diradicals could be transformed to ground state heat mediated by conical intersections (CI) that uniquely arise in diradicals as a result of the situation of the four energy states. This is the first time that full characterization of the processes taking place in PCE active diradicals is addressed, which is culminated with their efficient application in photodynamic action.

The GR→DR transition is forbidden by the one-photon optical selection rules as both states have the same symmetry in their spatial part wavefunctions. In closed-shell molecules (null diradical character) the energy sequence of the singlet states is GR<BR<DR in Scheme 1 and consequently, upon light absorption, internal conversion from high excited states ends up in the BR state (i.e., Kasha's rule) from which the molecule might eventually fluoresce.[10-11] The situation is different in diradicaloid systems, where the configurational mixing between the covalent and ionic states makes the DR state to decrease in energy in such a way that the energy ordering is reversed as GR<DR<BR. This results in a neat lack of optical emission response of the diradicals which are broadly known to be non-fluorescent materials. Mechanistically, some reports have ascribed the lack of fluorescence in diradicals to the existence of CI between these states, though these processes have been little explored or connected with photo-thermal properties.[12] This unique distribution of electronic states in diradicaloids has been exploited in singlet fission as the DR state can be viewed as the entangled intermediate triplet pair. In order to explore new functional capabilities in organic electronic applications, founded in the photo-physical properties imparted by the GR<DR<BR energy sequence of electronic states, we explore novel stable diradicaloids as photo-thermal conversion materials. Scheme 1D presents some of the most important small molecule chemical designs used in the literature of photo-thermal conversion ranging in PCE efficiencies of 70-80%.[13] A strategy is based on closed-shell molecules such as thiophene-based compounds with electron donor-acceptor-donor substitution pattern, or in cyanine cations; in these two cases, the PCE action is triggered by the strong light absorption properties in the NIR spectral region which is a critical requirement for biological applications of PCE molecules. Also, in Scheme 1D, it is included one of the few examples in the literature with the strategy of using open-shell diradical molecules (very small diradical character) as PCE units.[8] In the three cases, the key mechanism of energy conversion is assigned to the almost-free internal torsions in the conjugated backbone which are able to detune the PCE effect by efficient internal conversion.

Compared with other types of radicals, unpaired electrons of Blatter radicals can be widely delocalized, thus possessing unique electrical and magnetic properties such as antiferromagnetic or ferromagnetic interactions, spin π delocalization, narrow electrochemical windows, and low excitation energy.[14-21] More importantly, Blatter radicals show impressive stability lifetimes (over months) even in air. [22] In this article, we prepared a series of diradicaloids based on Blatter radicals designed with medium/large diradical character in order

This item was downloaded from IRIS Università di Bologna (https://cris.unibo.it/)

When citing, please refer to the published version.

to achieve such GR<DR<BR excited state ordering pursuing to obtain efficient photo-thermal organic-based materials. Double and triple bond bridges encapsulated by two Blatter based radicals or BDB and BTB in Figure 1 have been prepared, their photo-physical properties studied in-depth and finally implemented in photo-thermal studies which have shown outstanding conversion of 77.23%, one of the highest for radicaloid-based organic materials.[23-28] Encouragingly, photo-thermal agents based on BDB nanoparticles (NPs) exhibit excellent tumor cell-killing performance. [29-32]

Results and Discussion

This item was downloaded from IRIS Università di Bologna (https://cris.unibo.it/)

When citing, please refer to the published version.

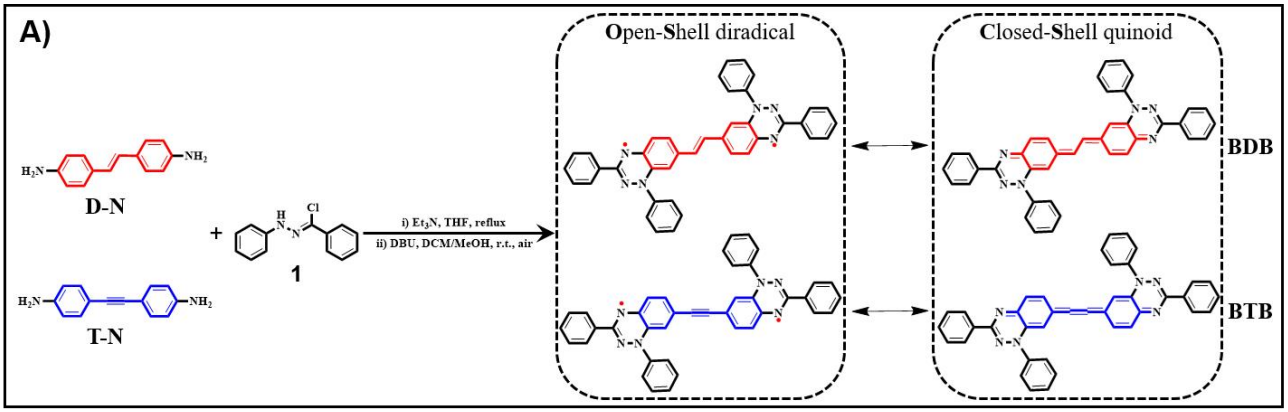

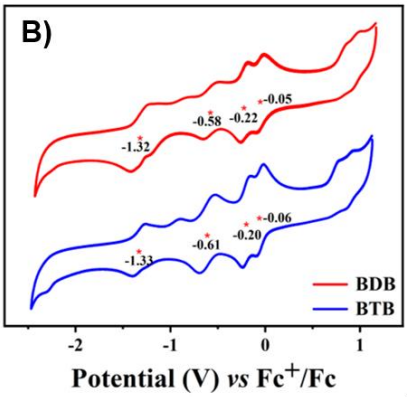

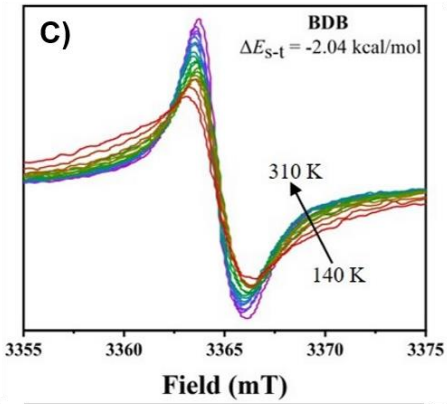

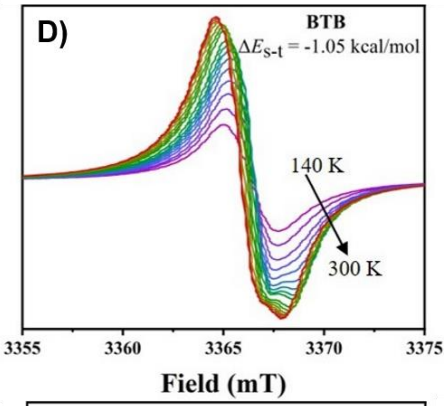

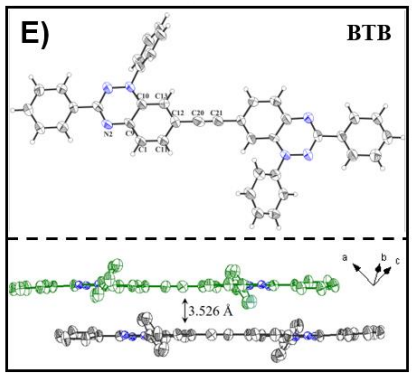

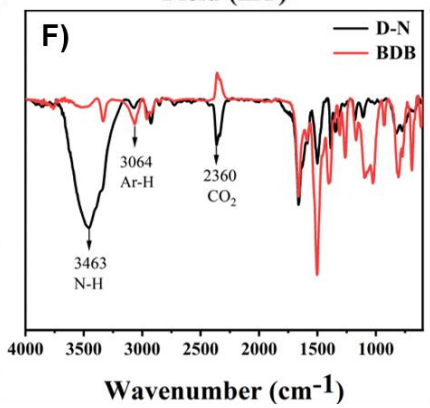

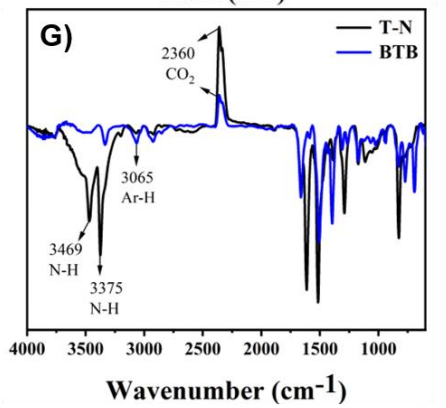

H) Summary of bond lengths (Å) for single crystal structure[a] and DFT calculation[b] of **BTB.**

	N2C9	C1C9	C9C10	C1C11	C10C13	C11C12	C12C13	C12C20	C20C21
BTB[a]	1.364	1.385	1.409	1.354	1.366	1.405	1.381	1.430	1.192
BTB[b]	1.354	1.413	1.428	1.376	1.393	1.418	1.406	1.413	1.215

Figure 1. (A) Synthesis and the resonance structures of BDB and BTB; (B) Cyclic voltammograms of BDB and BTB; (C) and (D) Variable temperature ESR spectra of BDB and BTB in benzophenone solid solution; (E) Single crystal structures and packing diagrams of BTB. Thermal ellipsoids are drawn at 50% Probability. Hydrogen atoms are omitted for clarity. Short contact (Å) is labelled; (F) and (G) FT-IR spectra of intermediates and diradicals; (H) Summary of bond lengths (Å) for single crystal structure and Density functional theory (DFT) calculation of BTB.

The target diradicals BDB and BTB are synthesized according to the steps shown in Figure 1a, and the synthetic details can be found in the supporting information. The corresponding intermediates are obtained by nucleophilic

This item was downloaded from IRIS Università di Bologna (https://cris.unibo.it/)

When citing, please refer to the published version.

substitution reaction of raw materials D-N and T-N with (*Z*)-1-[chloro(phenyl)-methylene]-2-phenyl-hydrazine **1**. Then, under the reaction of 1,8-diazabicyclo[5.4.0]undec-7-ene (DBU) and air, the Blatter diradicals BDB and BTB are obtained in reasonable yields. All diradicals are characterized by UV-vis-NIR spectroscopy, mass spectrometry, electron spin resonance (ESR) and Fourier transform infrared (FT-IR).

The electrochemical properties of these diradicals are measured by cyclic voltammetry (CV) in dry dichloromethane (DCM). As shown in Figure 1b, they all present multiple reversible

Table 1. Photophysical, electrochemical data, singlet-triplet energy gap ($\Delta E_{s\text{-}t}$), calculated diradical character (y_0) and photothermal conversion efficiency (η_{PT}) of BDB and BTB.

Comp.	HOMO[a] (eV)	LUMO[a] (eV)	E_g^{EC} [b] (eV)	λ_{max} (nm)	λ_{weak} (nm)	E_g^{Opt} [c] (eV)	$\Delta E_{s\text{-}t}^{Exp}$ [d] (kcal/mol)	y_0[e]	$\Delta E_{s\text{-}t}^{Cal}$ [e] (kcal/mol)	η_{PT} %
BDB	-4.22	-3.48	0.74	759	910	1.09	-2.04	0.616	-1.41	77.23
BTB	-4.19	-3.47	0.72	717	882	1.21	-1.05	0.695	-0.92	72.98

[a] HOMO and LUMO were calculated from cyclic voltammetry. [b] Eg^{EC}: electrochemical HOMO-LUMO energy gap. [c] Eg^{Opt}: optical energy gap estimated from the onset of absorption spectra. [d] ΔE_{s-t} was estimated by fitting the $I \cdot T$ versus T curves in Fig. S3 with the Bleaney-Bowers equation. [e] Calculated by quantum chemistry.

oxidation and reduction waves, and the half-wave potentials (*vs.* Fc^+/Fc) are calculated and marked with red stars in Figure 1. The highest occupied molecular orbitals (HOMO) and the lowest unoccupied molecular orbitals (LUMO) of these diradicals are calculated based on the half-wave potentials, and the electrochemical HOMO-LUMO energy gaps (E_g^{EC}) are further calculated (Table 1). BDB and BTB have four pairs of redox peaks, and their half-waves redox potentials are close, so they have similar HOMO and LUMO energy levels, -4.20 and -3.65 eV for BDB, and -4.24 and -3.54 eV for BTB, respectively.

Variable temperature ESR experiments have been carried out in benzophenone solid-state solutions such as shown in Figures 1c and 1d. ESR signal intensities in powder show an increase of the integrated signal with increasing temperature (Figure S3). The same behavior was found when the samples were dispersed in benzophenone what further excludes contributions by the interaction between molecules in the solid. The curves of *IxT* value versus temperature in Figure S3 are fitted with Bleaney-Bowers equation to estimate the singlet-triplet energy gap $\Delta E_{s\text{-}t}$ ($2J$) yielding $\Delta E_{s\text{-}t}$ values for BDB and BTB of -2.04 and -1.05 kcal/mol, respectively, indicating that the S_0 singlet ground state and the T_1 triplet low energy lying state are thermally connected by rather narrow gap as is typically found in diradicals with medium-large y_0. The diradical character, y_0, and the $\Delta E_{s\text{-}t}$ of the two molecules were calculated by quantum chemistry which amounts to be y_0=0.616 for BDB and for y_0=0.695 BTB, respectively.

The single crystals of BDB and BTB are grown by the slow solvent evaporation method of DCM solution for X-ray crystallographic analysis, only BTB obtained suitable crystal. The structure is shown in Figure 1e. The crystal system of the cell is triclinic, and the space group is $P\bar{1}$. Figure 1h provides detailed information on bond length. Interestingly, the bond length of C1-C11 and C10-C13 is shorter than that of conventional benzene ring, and the bond length of C12-C20 is shorter than that of ordinary single bond, which are due to the contribution of the quinoid closed-shell form (in agreement with the medium diradical character). The BTB molecule has a planar structure and forms a 1D stacking column with a distance of 3.526 Å.

In the FT-IR spectra (Figure 1f and 1g), from D-N (T-N) to BDB (BTB), the absence of typical N-H stretching vibration absorption above 3100 cm^{-1} indicates that the two BDB and BTB diradicals have good purity.

The optical absorption spectra of the Blatter diradicals in methyl-THF solutions are shown in Figure 2 and Table 1 summarizes the main values for the spectra in DCM. In methyl-THF, the main absorption band in BDB is a 778 nm (1.59 eV) and is due to the GR→BR excitation which shows a molar absorptivity of 2.54×10^3 M^{-1} cm^{-1} in line with the large oscillator strength due to the ionic character of the BR state. Replacing the double bond by a triple bond in the acetylene analogue, there is a blue-shift of the main absorption band up to 736 nm (1.68 eV). UV-Vis-NIR variable temperature experiments have been carried out to obtain a better resolution of the spectra, which is the particular case of the high energy part of these strongest absorption bands revealing a clear vibronic sequence of the GR→BR excitation. Two weak but perfectly resolved bands at 80 K at 930 nm (1.33 eV) and 1070 nm (1.16 eV) in BDB are observed which arise from the GR→DR excitation. The small absorbance of these bands is a consequence of the forbidden character of this transition which is slightly activated by vibronic borrowing from the strongly

This item was downloaded from IRIS Università di Bologna (https://cris.unibo.it/)

When citing, please refer to the published version.

allowed GR→BR band. In BTB, these weak bands are detected at 864 nm (1.44 eV) and 942 nm (1.32 eV) also blue-shifted

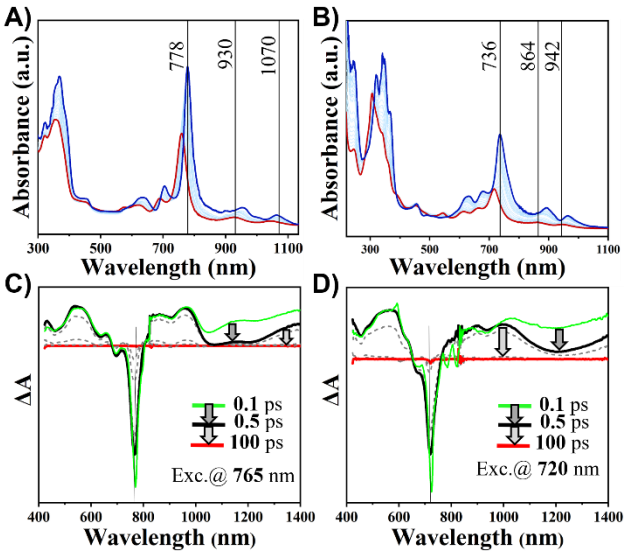

Figure 2. UV-vis-NIR absorption spectra of (A) BDB and (B) BTB in methyl-tetrahydrofuran (Methyl-THF) at 298 (red) and 80 (blue) K. Femtosecond transient absorption spectra for (C) BDB and (D) BTB in DCM at 0.1 ps (green), 0.5 ps (black), 1 ps (grey), 10 ps (grey) and 100 ps (red). Arrows denote the time evolution of the spectra.

compared to BDB. These weak excitations are characteristic of open-shell singlet diradicals and often described as the H,H → L,L excitation. [33] According to the position of these bands, the BR and DR states are very close in energy representing a favorable case not only for vibronic intensity borrowing but also for the appearance of conical intersections, such as discussed below.

Quantum chemical calculations at the (U)B3LYP and CASSCF (for optimization of the geometries, see Figures S4-S13) and NEVPT2 (for excitation energies) level have been carried out for the ground and excited states of BDB and BTB. For both molecules, the DR excited states are always predicted to be below the energy of the BR, such as observed experimentally, to different extent depending on the geometry chosen for the calculation. At the CASSCF optimized geometry of the ground state, for BDB the GR→BR transition is calculated at 1.83 eV (NEVPT2) and is measured at 1.59 eV whereas the GR→DR transition is predicted at 1.57 eV and measured at 1.33 eV. From calculations, the optical excitation is described as a HOMO→LUMO (i.e., H→L) transition whereas the lowest energy excitation is assigned to double HOMO,HOMO→LUMO,LUMO excitation (i.e., H,H→L.L where HOMO and LUMO topologies are shown in Figure 3). Similar to BTB, calculations predict the GR→DR band at 1.98 eV and the GR→BR excitation at 2.2 eV.

The emission properties of the two samples were probed at 80 and 298 K, respectively. But fluorescent spectra were not observed in any case. Figure 2 shows the results of the femtosecond transient absorption spectroscopy (fs-TAS) characterization for BDB and BTB in DCM at 298 K. All molecules show spectra, with excited state absorption (i.e., ESA) features both in the visible and in the NIR spectral regions, that decays with negligible time evolution from sample to sample (Figure S14), indicating the presence of similar single excited state species and mechanisms. All ESA bands disappear upon 100 ps in three steps: i) the optically absorbing BR singlet state species is first populated within 0.1 ps with distinctive NIR absorption bands; ii) the ESA bands of the BR state transform into a second ESA spectrum within 0.5 ps that could correspond to the population of the DR state in a ultrafast BR→DR non-radiative process; finally, iii) the DR singlet excited state quickly non-radiatively decays to the ground state, DR→GR, after few picoseconds, similarly to what is seen in literature for other diradical materials.[12] The deactivation after photoexcitation of BDT and BTB does not go through the alternative BR→GR channel given the absence of fluorescence which cannot compete with the described ultrafast decays. Hence, these transient features are consistent with the presence of an S_2→S_1 (BR→DR) internal conversion which is particularly efficient when the potential energy surfaces of the involved states have similar energies and geometries. For this transition, the possible existence of a conical intersection is not excluded since these appear in the typical cases when the state wavefunctions have similar energy/structures and different wavefunction symmetry (such as in BR and DR). Posterior DR→GR relaxation also occurs in subnanosecond times such as observed experimentally. This DR→GR takes place between state wavefunctions of the same symmetry invoking a similar situation to that reported for the photo-deactivation in antiaromatic

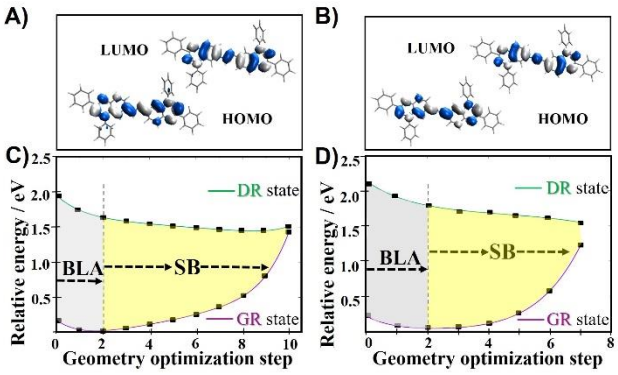

Figure 3. HOMO and LUMO orbitals of (A) BDB and (B) BTB at CASSCF level. GR and DR potential energy scans of (C) BDB and (D) BTB, following the optimization of the DR state and leading to a barrierless conical intersection with the GR state. The initial steps correspond to a motion along the CC BLA alternation coordinate followed by a symmetry breaking (SB) of the molecular structure leading to the conical intersection.

This item was downloaded from IRIS Università di Bologna (https://cris.unibo.it/)

When citing, please refer to the published version.

molecules happening between states of the same symmetry through the bond length alternation.[34] Nonetheless, both processes act in combination to convert all light-absorbed excitation energy into heat in a highly ultrafast manner.

To assess the last events in the photo-deactivation pathways, we attempted to optimize the geometry of the DR state at CASSCF level. As shown in Figure 3, the energy evolution of the DR state at CASSCF level shows an initial decrease corresponding to a motion along the BLA alternation coordinate followed by a symmetry breaking that leads to a barrierless crossing of the GR and DR states, without reaching a stable DR structure. Notably, the optimization of the DR state, initially follows a bond length alternation coordinate in which for the central double bond distance of the oligoene spacer between the Blatter units is shortened and the single bonds enlarged. Due to the delocalized orbital nature (Figures 3a and 3b), also the Blatter units undergo remarkable geometry changes. In these first stages, the calculations predict a moderate destabilization of the GR state which is concomitant with an energy lowering of the DR excited state. The interesting point is that after the initial BLA changes, the molecular structure starts breaking its symmetry and the DR state lowers its energy without overcoming an energy barrier. At the same time, such symmetry breaking leads to an abrupt increase of the GR state energy and the two potential energy curves intercept each other, with the feature that both potential energy lines cross before an energy minimum for the DR is found (Figure 3c). This is a clear indication that the two states are connected by a conical intersection at the crossing point between the two states, which is reached barrierless after the population of the DR state. The presence of a conical intersection between the ground and the lowest excited energy state of the same symmetry is not common. The presence of such CI between same symmetry states has been described for antiaromatic systems in which such processes are characterized by a change of the BLA path between the involved states as well as a change in the sign of the wavefunction.[34] According to our calculation such change in the

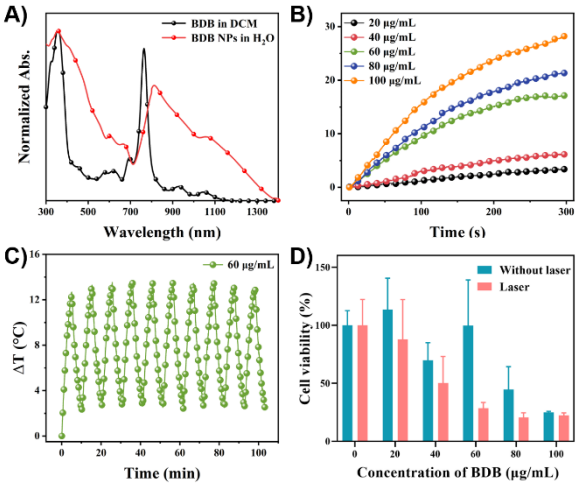

Figure 4. (A) Absorption spectra of BDB in DCM and BDB NPs in water; (B) Photothermal conversion of BDB NPs at different concentrations (20-100 μg/mL) under 808 nm laser irradiation (1.2 W cm^{-2}); (C) Photothermal stability study of BDB NPs during ten circles of heating-cooling processes; (D) Viabilities of the 4T1 cells determined by CCK8 assay after incubation at various concentrations of BDB-PEG with or without 808 nm laser irradiation (1.2 W cm^{-2}, 5 min).

BLA pattern is also found between the central oligoene bridge on going from GR to DR. The same calculations have been carried out for BTB in which we found out very similar results including the appearance of the CI between the DR and GR states with a similar pattern as in BDB: initially the geometry of the DR state changes along the BLA coordinate and then a symmetry breaking occurs leading to the CI (Figure 3d).

These excited state descriptions and connections inspired us to study their photo-thermal properties. It is worth noting first that the absorption of BDB and BTB in solid state powders can be further expanded into the second region of the NIR spectrum with neat absorbances from 300 to 1400 nm, such as shown in Figure S15. Under the irradiation with the 808 nm laser (0.8 W cm^{-2}), the surface temperature of BDB and BTB powders rapidly rises to about 140 °C within 25 s, and then quickly returns to room temperature after stopping laser irradiation, showing an efficient photo-thermal conversion process. After repeated whole cycles (Figure S15) of heating and cooling processes, scarce changes of the photothermal responses are observed which suggested the excellent photo-stability of Blatter-based diradicals. Importantly, the photothermal conversion efficiencies of BDB and BTB under 808 nm laser are calculated as high as 77.23 % and 72.98 %, indicating that they have excellent photo-thermal properties. To the best of our knowledge, BDB possesses one of the highest photo-thermal conversion efficiency for diradical-based materials reported in the literature.

This item was downloaded from IRIS Università di Bologna (https://cris.unibo.it/)

When citing, please refer to the published version.

Due to the excellent photothermal conversion efficiency of BDB, we have tried to use it as a photothermal agent (PTA) to kill cancer cells using its local heating generated under visible or NIR light. BDB is encapsulated by the amphiphilic copolymer 1,2-distearyl-sn-glycerol-3-phosphate ethanolamine-*N*-[hydroxy (polyethylene glycol)-2000] (DSPE-PEG_{2000}) and prepared into polymer nanoparticles (NPs).[35] The NIR absorption of BDB NPs is measured (Figure 4a), showing a red shift compared to the absorption in DCM solution, with strong absorption around 812 nm. By testing the photothermal conversion of BDB NPs at different concentrations under 808 nm laser irradiation (1.2 W cm^{-2}), it is found that the solution temperature could be significantly increased within 300 seconds (Figure 4b). More importantly, BDB NPs solution (60 μg/mL) did not degrade after 10 cycles of heating and cooling under continuous laser irradiation (Figure 4c), demonstrating excellent chemical, thermal and photostability, and laying the foundation for subsequent cell experiments.

The cytotoxicity and phototoxicity of BDB-PEG to 4T1 cancer cells are evaluated by CCK8. Figure 4d shows that the cell viability decreased with increasing the BDB-PEG concentration, suggesting the cytotoxicity of as-prepared free radicals NPs to cancer cells. Meanwhile, a more significant therapeutic effect can be observed after irradiation (1.2 W cm^{-2}) with 808 nm laser for 5 min. The results indicated that the photothermal effect of the BDB-PEG in cancer cells could be triggered by NIR irradiation, and the laser-triggered photothermal effect exhibited a satisfactory performance of tumor cell-killing at the concentration of 60 μg/mL.

Conclusion

The understanding of the energy distribution of the lowest energy lying excited states in diradicals tells us that the main optical and photonic properties are dictated by the mixing between the ground electronic state and the same symmetry second ionic state. This produces the appearance of tunable diradical character in the ground state and low energy lying triplet excited states. The description of the interplay between low and high spin state in such diradicals have been extensively studied. However, much less knowledge and efforts have been devoted to the understanding of the photophysics between the two higher energy states and the ground state. We now describe that in despite of the GR and the DR share the same symmetry they are connected by a conical intersection. This has been revealed in a series of diradical based on Blatter unit covalently connected with oligoene and oligoyne bridges which possess medium-high diradical character, have strong oscillator strength for the main optical absorption band and its lowest energy singlet excited state is a one-photon forbidden state which is coupled by a CI to the ground state. This makes these molecules ideal chromophores for intense light absorption in the NIR region and efficient molecules to convert the absorbed light energy into heat by CI deactivation as confirmed by the very high photo-thermal conversion efficiencies which range among the largest described for diradicals and radicals. Furthermore, diradical BDB is applied to photothermal therapy of tumor cells with good stability and satisfactory performance.

Supporting Information

The authors have cited additional references within the Supporting Information.

Acknowledgements

The authors acknowledge the financial support from the National Natural Science Foundation of China (22375029), the Open Research Fund of Chengdu University of Traditional Chinese Medicine State Key Laboratory Southwestern Chinese Medicine Resources (SKLTCM2022014), Intelligent Terminal Key Laboratory of Sichuan Province (SCITLAB-20012 and SCITLAB-20013), Guangdong Basic and Applied Basic Research Foundation (2021A1515110431) and the National Natural Science Foundation of China (52203134). We thank MINECO/ FEDER of the Spanish Government (PID2021-127127NB-I00), the Junta de Andalucía of Spain (PROYEXCEL-0328) and Research Central Services (SCAI) of the University of Málaga for the access to the facilities. RFO funds from the University of Bologna, Italy, are also acknowledged.

Keywords: Radicals • Blatter-Type Diradicals • Excited States • Photo-thermal Conversion • Photophysics

[1] a) L. Salem, C. Rowland, *Angew. Chem. Int. Ed*. **1972**, *11*, 92-111; b) V. Bonačić-Koutecký, J. Koutecký, J. Michl, *Angew. Chem. Int. Ed*. **1987**, *26*, 170-189.

[2] a) Y. H. Zheng, M. S. Miao, G. Dantelle, N. D. Eisenmenger, G. Wu, I. Yavuz, M. L. Chabinyc, K. N. Houk, F. Wudl, *Adv. Mater.* **2015**, *27*, 1718-1723. b) Y. Zhang, Y. H. Zheng, H. Q. Zhou, M. S. Miao, F. Wudl, T. Q. Nguyen, *Adv. Mater.* **2015**, *27*, 7412-7419.

[3] G. E. Rudebusch, J. L. Zafra, K. Jorner, K. Fukuda, J. L. Marshall, I. Arrechea-Marcos, G. L. Espejo, R. P. Ortiz, C. J. Gómez-García, L. N. Zakharov, M. Nakano, H. Ottosson, J. Casado, *Nat. Chem.* **2016**, *8*, 753-759.

[4] S. Mori, S. Moles Quintero, N. Tabaka, R. Kishi, R. Gónzalez Núñez, A. Harbuzaru, R. Ponce Ortiz, J. Marín-Beloqui, S. Suzuki, C. Kitamura, C. J. Gómez-García, Y. Dai, F. Negri, M. Nakano, S. Kato, J. Casado, *Angew. Chem. Int. Ed*. **2022**, *61*, e202206680.

[5] D. Yuan, D. Huang, S. Medina Rivero, A. Carreras, C. Zhang, Y. Zou, J. Jiao, C. R. McNeil, X. Zhu, C. Di, D. Zhu, D. Casanova, J. Casado, *Chem*. **2019**, 5, 964-976.

[6] a) H. Hayashi, J. E. Barker, A. Cárdenas Valdivia, R. Kishi, S. N. MAcMillan, C. J. Gómez-García, H. Miyauchi, Y. Nakamura, M. Nakano,

This item was downloaded from IRIS Università di Bologna (https://cris.unibo.it/)

When citing, please refer to the published version.

S. Kato, M. M. Heley, J. Casado, *J. Am. Chem. Soc*. **2020**, *142*, 20444-20455. b) J. J. Dressier, A. Cárdenas Valdivia, R. Kishi, M. Nakano, J. Casado, M. M. Haley, *Chem*, **2020**, *6*, 1353-1368.

[7] G. Y. Chen, J. M. Sun, Q. Peng, Q. Sun, G. Wang, Y. J. Cai, X. G. Gu, Z. G. Shuai, B. Z. Tang, *Adv. Mater.* **2020**, 1908537.

[8] Z. J. Wang, J. W. Zhou, Y. H. Zhang, W. Y. Zhu, Y. Li, *Angew. Chem. Int. Ed.* **2022**, *134*, e202113653.

[9] H. Q. Li, X. L. Zou, H. J. Chen, W. R. Lian, H. Y. Jia, X. H. Yan, X. G. Hu, X. Y. Liu, *Adv. Opt. Mater.*, **2023**, DOI: 10.1002/adom.202300060.

[10] J. Li, W. Zhang, W. H. Ji, J. Q. Wang, N. X. Wang, W. X. Wu, Q. Wu, X. Y. Hou, W. B. Hu, L. Li, *J. Mater. Chem. B*, **2021**, *9*, 7909-7926.

[11] X. L. Weng, J. Y. Liu, *Drug Discov. Today*, **2021**, *26*, 2045-2052.

[12] B.D. Rose, L.E. Shoer, M. R. Wasielewski, M. M. Haley, *Chem.Phys. Lett*., **2014**, *616-617*, 137-141.

[13] B. Guo, Z. M. Huang, Q. Shi, E. Middha, S. D. Xu, L. Li, M. Wu, J. W. Jiang, Q. L. Hu, Z. W. Fu, B. Liu, *Adv. Funct. Mater.* **2020**, *30*, 1907093.

[14] C. P. Constantinides, A. A. Berezin, M. Manoli, G. M. Leitus, G. A. Zissimou, M. Bendikov, J. M. Rawson, P. A. Koutentis, *Chem. Eur. J.* **2014**, *20*, 5388-5396.

[15] C. P. Constantinides, A. A. Berezin, G. A. Zissimou, M. Manoli, G. M. Leitus, M. Bendikov, M. R. Probert, J. M. Rawson, P. A. Koutentis, *J. Am. Chem. Soc.* **2014**, *136*, 11906-11909.

[16] F. A. Neugebauer, G. Rimmler, *Magn. Reson. Chem.* **1988**, *26*, 595-600.

[17] A. A. Berezin, C. P. Constantinides, S. I. Mirallai, M. Manoli, L. L. Cao, J. M. Rawson, P. A. Koutentis, *Org. Biomol. Chem.* **2013**, *11*, 6780-6795.

[18] F. A. Neugebauer, I. Umminger, *Chem. Ber.* **1980**, *113*, 1205-1225.

[19] N. M. Gallagher, J. J. Bauer, M. Pink, S. Rajca, A. Rajca, *J. Am. Chem. Soc.* **2016**, *138*, 9377-9380.

[20] S. Y. Zhang, M. Pink, T. Junghoefer, W. C. Zhao, S. N. Hsu, S. Rajca, A. Calzolari, B. W. Boudouris, M. B. Casu, A. Rajca, *J. Am. Chem. Soc.* **2022**, *144*, 6059-6070.

[21] F. J. M. Rogers, P. L. Norcott, M. L. Coote, *Org. Biomol. Chem.* **2020**, *18*, 8255-8277.

[22] F. A. Neugebauer, I. Umminger, *Chem. Ber.* **1981**, *114*, 2423-2430.

[23] X. G. Hu, H. J. Chen, L. Zhao, M. S. Miao, X. L. Zheng, Y. H. Zheng, *J. Mater. Chem. C* **2019**, *7*, 10460-10464.

[24] X. G. Hu, H. J. Chen, L. Zhao, M. S. Miao, J. Y. Han, J. Wang, J. Guo, Y. Y. Hu, Y. H. Zheng, *Chem. Commun.* **2019**, *55*, 7812-7815.

[25] X. G. Hu, H. J. Chen, G. D. Xue, Y. H. Zheng, *J. Mater. Chem. C* **2020**, *8*, 10749-10754.

[26] Y. Ji, L. X. Long, Y. H. Zheng, *Mater. Chem. Front.* **2020**, *4*, 3433.

[27] F. Miao, Y. Ji, B. Han, S. M. Quintero, H. J. Chen, G. D. Xue, L. L. Cai, J. Casado, Y. H. Zheng, *Chem. Sci.* **2023**, *14*, 2698-2705.

[28] T. T. Sun, J. X. Guo, H. Wen, Q. Pei, Q. H. Wu, D. Y. Hao, C. D. Dou, Z. G. Xie, *Aggregate*. **2023**, DOI:10.1002/agt2.362.

[29] X. M. Cui, Q. F. Ruan, X. L. Zhuo, X. Y. Xia, J. T. Hu, R. F. Fu, Y. Li, J. F. Wang, H. X. Xu, *Chem. Rev.* **2023**, DOI: 10.1021/acs.chemrev.3c00159.

[30] D. M. Xi, M. Xiao, J. F. Cao, L. Y. Zhao, N. Xu, S. R. Long, J. L. Fan, K. Shao, W. Sun, X. H. Yan, X. J. Peng, *Adv. Mater.* **2020**, *32*, 1907855.

[31] C. L. Anderson, T. Zhang, M. Qi, Z. M. Chen, C. Q. Yang, S. J. Teat, N. S. Settineri, E. A. Dailing, A. Garzón-Ruiz, A. Navarro, Y. Q. Lv, Y. Liu, *J. Am. Chem. Soc.* **2023**, *145*, 5474–5485.

[32] Z. Zhao, C. Chen, W. T. Wu, F. F. Wang, L. L. Du, X. Y. Zhang, Y. Xiong, X. W. He, Y. J. Cai, R. T. K. Kwok, J. W. Y. Lam, X. K. Gao, P. C. Sun, D. L. Phillips, D. Ding, B. Z. Tang, *Nat. Commun.* **2019**, *10*, 768.

[33] S. Canola, J. Casado, F. Negri, *Phys. Chem. Chem. Phys*. **2018**, *20*, 24227–24238.

[34] S. Zilberg, Y. Haas, *Chem. Eur. J*. **1999**, *5*, 1755– 1765.

[35] H. X. Yuan, Z. L. Li, Q. Zhao, S. C. Jia, T. Wang, L. Xu, H. T. Yuan, S. L. Li, *Adv. Funct. Mater.* **2023**, *33*, 2213209.

This item was downloaded from IRIS Università di Bologna (https://cris.unibo.it/)

When citing, please refer to the published version.

Entry for the Table of Contents

A conical intersection between the lowest energy excited state and the ground state of the Blatter-type diradical is responsible for highly efficient light-to-heat conversion of the absorbed radiation. Also, it is first applied to photothermal therapy of tumor cells, demonstrating good stability and the highest photo-thermal conversion in the diradicaloid field.

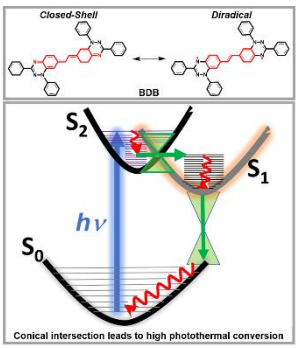

77% Photothermal Conversion in Blatter-Type Diradicals: Photophysics and Photodynamic Applications

Y. Ji, S. Quintero, Y. Dai, J. Beloqui, H. Zhang, Q. Zhan, F. Sun, D. Wang, X. Li, Z. Wang, X. Gu, F. Negri, J. Casado, Y. Zheng

This item was downloaded from IRIS Università di Bologna (https://cris.unibo.it/)

When citing, please refer to the published version.